Phase transitions and relaxation dynamics in (NH4I)x(KI)1-x mixed crystals

F. Güthoff, Michael Ohl, Manfred Reehuis, Alois Loidl

Angaben zur Veröffentlichung / Publication details:

Güthoff, F., Michael Ohl, Manfred Reehuis, and Alois Loidl. 1999. "Phase transitions and relaxation dynamics in (NH4I)x(KI)1-x mixed crystals." *Physica B* 266 (4): 310–20. https://doi.org/10.1016/S0921-4526(99)00049-6.

Phase transitions and relaxation dynamics in $(NH_4I)_x(KI)_{1-x}$ mixed crystals

F. Güthoff[a], M. Ohl[b,*], M. Reehuis[b,c], A. Loidl[b]

[a]*Institut für Festkörperforschung, Forschungszentrum Jülich GmbH, D-52425 Jülich, Germany*
[b]*Experimentalphysik V/EKM, Institut für Physik, Universität Augsburg, Universitätsstr. 1, D-86159 Augsburg, Germany*
[c]*BENSC, Hahn–Meitner-Institut, Glienicker Str. 100, D-14109 Berlin, Germany*

1. Introduction

As a function of temperature and pressure the ammonium halides NH_4X (X = Cl, Br and I) undergo a sequence of order–disorder phase transitions [1]. All NH_4X compounds reveal a high-temperature plastic phase, which is dynamically disordered and characterized by an almost free reorientational motion of the NH_4^+-ions. This rotor phases reveal an NaCl-type structure (α-phase). On decreasing temperature (or increasing pressure) this phase is followed by a CsCl-structure (β-phase) in

* Corresponding author. Tel.: + 49-821-598-3606; fax: + 49-821-598-3649.
E-mail address: michael.ohl@physik.uni-augsburg.de (M. Ohl)

which the NH_4^+-tetrahedra reorient between two symmetry-equivalent positions [2]. The temperature of the αβ-phase transition, $T_{\alpha\beta}$, critically depends on the size (polarizability) of the halogen ions and is highest for X = Cl and lowest for X = I. In the γ-phase, which is of tetragonal symmetry and is the stable low-temperature phase of NH_4I, full orientational order is achieved in a slightly distorted CsCl-structure.

It is already known [3] that NH_4I and KI are completely miscible. In the mixed-crystal system $(NH_4I)_x(KI)_{1-x}$, with increasing potassium concentration the phase transitions into orientationally long-range ordered phases are shifted to lower temperatures and finally become fully suppressed [4,5]. In a narrow concentration range, $0.55 \leqslant x \leqslant 0.75$, a new trigonal low-temperature structure (ε-phase) has been detected [6]. This phase shows long-range order of the NH_4^+-tetrahedra with two inequivalent ammonium sites. For $x < 0.55$ a random freezing in of the orientational degrees of freedom occurs [4,7,8]. This collective freezing process of reorienting moments into random configurations is the well known orientational-glass transition [9]. For many years these orientational glasses (OG) served as conceptual links between phase and glass-transition phenomena.

In the present paper we report detailed elastic and quasielastic neutron-scattering experiments on $(NH_4I)_x(KI)_{1-x}$ mixed crystals with ammonium concentrations $x = 0.55$, 0.65, 0.75 and 0.80. To characterize the mixed crystals and to study the dipolar relaxation dynamics, these experiments were accompanied by measurements of the dielectric loss function. The main aim of this work was the study of the relaxation dynamics in the ε-phase. In this phase two time constants, characteristic for two different relaxational processes, have been detected in dielectric spectroscopy [4] and it seemed highly interesting if two time scales also show up in neutron-scattering experiments.

2. Sample preparation and experimental details

2.1. Sample preparation and characterization

All crystals were grown from aqueous solutions. As-grown crystals had a size of approximately 1 cm^3, they were transparent with a cleavage plane parallel to (1 0 0). The concentrations used throughout this text are the concentrations as prepared in the aqueous solutions. To determine the actual ammonium concentrations in the crystals we focused on the concentration dependence of the lattice constants using X-ray diffraction techniques at room temperature. To achieve higher accuracy only crushed single crystals were used. For comparison we determined the lattice constants of the pure compounds KI and NH_4I and, assuming Vegard's law [10], we calculated the lattice constant as a function of ammonium concentration according to $a(x)\ [\text{Å}] = (7.067 + 0.198 * x)\ [\text{Å}]$. This result is close to those previously reported [6,11]. Fig. 1 shows the concentration dependence of the lattice constant as calculated using the equation above (solid line) and is compared with the lattice constants as measured for a given concentration x of the aqueous solution (solid triangles). At intermediate concentrations significant discrepancies appear which amount to almost 5%, with the actual ammonium concentration in the crystal being lower than in the aqueous solution. But it seems also worth to mention that the discrepancies between the ammonium concentrations in the solid and the aqueous solutions is much smaller as reported previously. This is the result of improved growing conditions where we grew small crystals from a large amount of aqueous solutions.

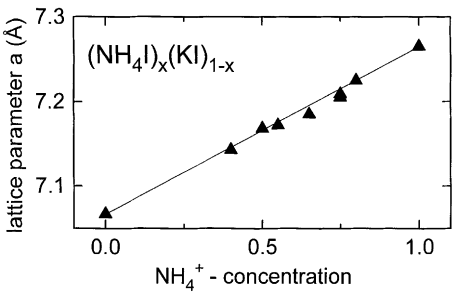

Fig. 1. Room-temperature lattice parameters obtained from X-ray diffraction as a function of the NH_4^+-concentration in the aqueous solution. The solid line is a linear extrapolation (Vegard's law) of the lattice constants of the pure compounds KI and NH_4I.

2.2. Experimental details

Neutron-scattering experiments were performed using the four-circle diffractometer E5 and the triple-axis spectrometer E7 (TAS) at the thermal source of the BER II reactor at the Hahn–Meitner-Institut in Berlin. For the inelastic measurements on the triple-axis spectrometer a fixed incoming wavelength of $\lambda_i = 2.38$ Å was chosen. For $x = 0.55$, 0.65, and 0.75 collimations of 40′-20′-20′-30′ were used. The energy resolution in this configuration was of the order of $\Delta E \cong 115$ GHz. For $x = 0.80$ the collimations were set to 60′-40′-40′-60′, yielding an energy resolution $\Delta E \cong 195$ GHz. The resolution in momentum transfer was approximately $\Delta Q = 0.025$ Å^{-1} for $x = 0.55$, 0.65 and 0.75 and amounted 0.04 Å^{-1} for $x = 0.80$. The resolution was determined from vanadium constant-Q scans. Typical sample volumes for the E7 experiments were at least 1 cm^3 and the temperature stability was $\Delta T < 0.25$ K utilizing standard orange-type cryostats. At the four-circle diffractometer E5 a copper monochromator (Cu 220) selected an incoming wavelength of $\lambda_i = 0.924$ Å. The data were collected with a two-dimensional position-sensitive ^{3}He-detector with dimensions of 90×90 mm^2. The single crystals used for the elastic measurements were cut from as-grown crystals and had a typical size of $0.4 \times 0.4 \times 0.4$ cm^3. The samples were mounted in a two-stage closed-cycle refrigerator. The stability of the temperature was better than $\Delta T < 0.2$ K.

Additionally, dielectric measurements from room temperature down to 4 K were carried out, with a temperature stability better than $\Delta T <$ 0.5 K. Heating and cooling rates of roughly 0.4 K/min have been chosen. For these experiments the crystals were cleaved into small pieces along a plane parallel to (1 0 0) with dimensions $7 \times 6 \times 1$ mm^3. Gold electrodes were prepared by sputtering techniques. The use of gold was essential due to its non-reactive character with the I^--ions. We measured the temperature dependence of the complex dielectric function $\varepsilon = \varepsilon' - i\varepsilon''$ for frequencies 20 Hz $\leqslant \nu \leqslant$ 1 MHz using standard LCR meters and home-built He-flow cryostats.

3. Experimental results

3.1. Dielectric spectroscopy

The dielectric measurements on $(NH_4I)_x(KI)_{1-x}$ were performed to characterize the mixed crystals, to study the phase transitions and to complete the phase diagram. Here we present results of the temperature dependence of the complex dielectric function $\varepsilon = \varepsilon' + i\varepsilon''$ for the investigated samples. Fig. 2 shows the temperature dependence of the dielectric constant ε' (upper panel) and the dielectric loss ε'' (lower panel) at a fixed measuring frequency $\nu = 100$ kHz for the concentrations $x = 0.55$, 0.65 and 0.75. For $x = 0.80$ the dielectric constant as a function of temperature is hard to interpret [4]. $\varepsilon'(T)$ shows a step-like decrease at approximately 80 K with large hysteresis effects indicative for a first-order martensitic phase transition from the NaCl-type α-phase to the CsCl-type β-phase. $\varepsilon''(T)$ is always zero within the experimental uncertainties. From this observation and from the fact that

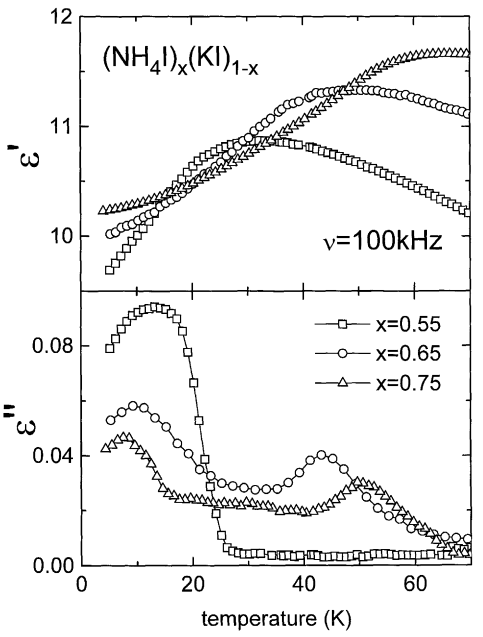

Fig. 2. Temperature dependence of the dielectric constant ε' (upper panel) and the dielectric loss ε'' (lower panel) for different ammonium concentrations $x = 0.55$, 0.65 and 0.75 at a fixed measuring frequency $\nu = 100$ kHz.

the crystals once cooled below 80 K stay opaque even after some heating cycles, we conclude that mixed crystals with ammonium concentration $x = 0.80$ ($a = 7.225$ (3) Å) pass through the αβ-phase transition at higher temperatures, but from the neutron-scattering experiments we will demonstrate later that the stable low-temperature structure is the ε-phase.

As the relevant physical aspects are easier to interpret in the loss functions we will discuss $\varepsilon''(T)$ at first. For $x = 0.65$ and 0.75 the dielectric loss provides clear experimental evidence for two anomalies. One located at approximately 10 K independent of concentrations and one located at 42 K for $x = 0.65$ and 50 K for $x = 0.75$. Interestingly, only one loss anomaly at low temperatures can be detected for $x = 0.55$. However, this anomaly seems to be considerably broadened and it has been concluded earlier that the two anomalies, which are well separated at higher concentrations, just have merged at an ammonium concentration $x = 0.55$ [4]. From this experimental fact we conclude that the time scales of both relaxational processes are close to the time window set by the dielectric experiment. Hence, two clearly separated anomalies can be detected only for the concentrations $x = 0.65$ and 0.75 which are expected to reveal the ε-phase at low temperatures. For $x = 0.80$ the ε-phase is the stable low-temperature structure, but the system passes through a first-order martensitic phase transition at higher temperatures, while for $x = 0.55$ the molecular orientations freeze-in despite of long-range orientational order. The temperature dependence of the dielectric constant $\varepsilon'(T)$ (upper panel of Fig. 2) is not so elucidative. It reveals one broad cusp which shifts to lower temperatures as the ammonium concentration decreases.

It is important to conclude from this section that the dielectric loss in crystals revealing the pure ε-phase shows two anomalies, corresponding to two distinctly different time scales in the relaxation dynamics at a given temperature. It has been concluded earlier [4] that the high-temperature anomaly possibly signals critical fluctuations at the αε-phase transition temperature, while the low-temperature anomaly could be related to a remaining residual reorientational motion of the ammonium molecules.

3.2. Neutron – scattering results

3.2.1. Neutron diffraction

To investigate the orientational-glass state and to detect possible traces of the ε-phase at the phase boundary between the stable ε-phase and the glass phase, the mixed crystal $(NH_4I)_{0.55}(KI)_{0.45}$ was investigated at $T = 11$ K and $T = 295$ K by single-crystal neutron-diffraction techniques. More than 400 reflections were recorded at each temperature. To improve the precision in the integration of the weak diffraction peaks, they were integrated by a method which uses the parameters describing the shapes of strong peaks. This procedure minimizes the relative standard deviations $\sigma(I)/I$ [12]. The crystal structure refinements were carried out with the full-matrix least-squares program CRYLSQ of the XTAL suite. The neutron-scattering lengths $b(H) = -3.7409$ fm, $b(N) = 9.36$ fm, $b(K) = 3.71$ fm and $b(I) = 5.28$ fm were used [13]. The measurement and refinement parameters of the single-crystal diffraction studies are listed in Table 1. At both temperatures no additional Bragg reflections, characteristic for the ε-structure, were detected. Therefore, the refinements were carried out in the space-group Fm $\bar{3}$ m using the model C of reference [6]. Here the NH_4^+-tetrahedra are statistically disordered over eight symmetry-equivalent orientations; three hydrogen atoms are in the

Table 1
Measurement and refinement parameters of the single-crystal diffraction studies of $(NH_4I)_{0.55}(KI)_{0.45}$ at 11 and 295 K

Temperature (K)	11	295
Neutron wavelength (Å)	0.924	0.924
Space group	Fm $\bar{3}$ m	Fm $\bar{3}$ m
No. of molecules per unit cell	4	4
No. of data recorded	568	411
Lattice parameter a (Å)	7.108(1)	7.175(1)
No. of unique data	69	70
No. of data used for refinement[a]	543	406
No. of variable parameters	9	9
θ range	6.3–50.8	6.3–50.8
$R(F)$	0.045	0.056
$R_w(F)$	0.024	0.022

[a] Symmetrically equivalent reflections with more than 6σI from the average were rejected.

Wyckoff position 96 k ($x\ x\ z$) while the fourth hydrogen atom is in the position 32f ($x\ x\ x$). With this model the crystal structure was successfully refined. At $T = 11$ K the isotropic thermal parameters of the N and K atoms were constrained to be equal, while in the case of the data set measured at $T = 295$ K the thermal parameters of the hydrogen atoms H1 and H2 were constrained to be equal. For both data sets the extinction parameters g were refined to values close to zero and were finally neglected. The results are summarized in the Table 2. At room temperature, as well as at $T = 11$ K the structural refinements yield the ideal cubic structure and even the thermal parameters are strongly reduced as a function of temperature. No clear experimental evidence for strong local distortions which would produce large "static" Debye–Waller factors, as observed in a number of OG [14,15], could be detected and from the neutron diffraction point of view, $(NH_4I)_{0.55}(KI)_{0.45}$ displays the features of a normal mixed molecular crystal.

We state that we have chosen similar measurement and refinement conditions on the same diffractometer compared to those in Ref. [6], in which in the crystal $(NH_4I)_{0.73}(KI)_{0.27}$ the ε-phase was established. The question remains why we could not detect this structure for an ammonium concentration $x = 0.55$, in which the ε-phase still should exist [5]. We conclude that the pure Bragg reflections indicative for the ε-phase with long-range order (LRO) do not exist. It will be documented in the next section that this concentration apparently shows short-range order (SRO) of the ε-phase. This SRO appears at the borderline to the orientational-glass phase.

3.2.2. Elastic studies at a triple-axis spectrometer

In these elastic measurements we wanted to gain insight into the "static" properties of the ε-phase as a function of the ammonium concentration x. Thus, we collected a series of Q-scans at zero-energy transfer at the (3 0 0) reciprocal lattice point (rlp). The appearance of this Bragg reflection is a fingerprint of the ε-phase and we tried to find experimental evidence for precursor effects or for the possible existence of finite correlation lengths indicative for short-range order (SRO). Hence we measured the temperature dependence of the Q-scans at zero-energy transfer at the superstructure reflection (3 0 0) along (ξ 0 0) for all investigated concentrations. In Fig. 3 we plotted some representative scans covering all samples $x = 0.55$ (Fig. 3a), 0.65 (Fig. 3b), 0.75 (Fig. 3c) and 0.80 (Fig. 3d). In all four spectra of Fig. 3 the ε-type structure clearly can be detected. A second peak at the position (3.05, 0, 0) can be ascribed to the (111) reflection of the aluminum sample holder. The full-width at half-maximum (FWHM) of this Bragg reflection indicates the instrumental resolution. Gaussian distribution functions fitted the data reasonably well. The dashed lines represent the fits of the (3 0 0) reflection and dotted lines indicate the fits to the aluminum profiles.

Already a rough inspection of Fig. 3 indicates that well-defined Bragg peaks, which indicate the stable ε-phase with long-range order (LRO), can be identified in crystals with concentrations $x = 0.65$

Table 2
Atomic coordinates and mean square displacement parameters of the single-crystal diffraction study in $(NH_4I)_{0.55}(KI)_{0.45}$ at $T = 11$ K and $T = 295$ K. Standard deviation in the values of the last significant digits are given in parenthesis. The isotropic thermal parameters U(Å^2) are of the form $\exp(-8/\pi^2\ (\sin^2(\theta_{hkl})/\lambda^2)$

Atom	Fm $\bar{3}$ m	11 K				295 K			
		x	y	z	U	x	y	z	U
I	4a	0	0	0	0.0062(4)	0	0	0	0.049(1)
N	4b	0.5	0.5	0.5	0.0097(4)	0.5	0.5	0.5	0.028(7)
K	4b	0.5	0.5	0.5	0.0097(4)	0.5	0.5	0.5	0.11(1)
H1	32f	0.575(2)	0.575	0.575	0.045(6)	0.573(3)	0.573	0.573	0.079(6)
H2	96k	0.5242(9)	0.5242	0.3553(10)	0.024(2)	0.527(3)	0.527	0.3635(15)	0.079(6)

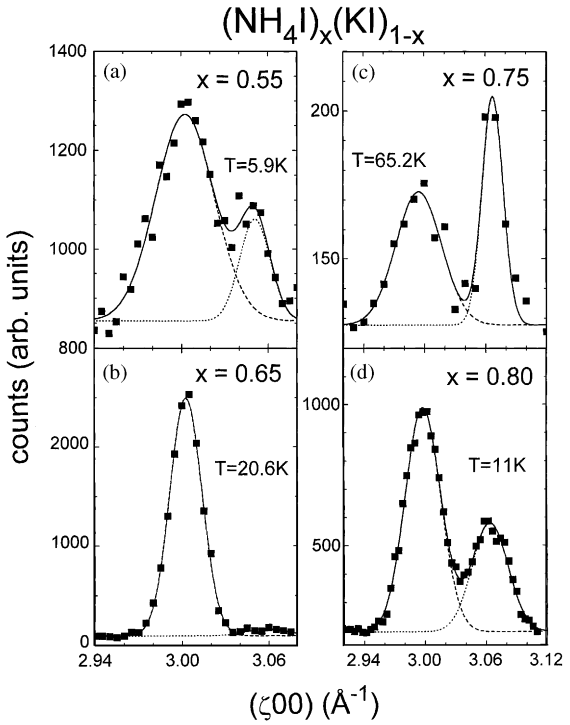

Fig. 3. Q-scans at zero-energy transfer at the (3 0 0) rlp along the [ξ 0 0] direction for different ammonium concentrations x at various temperatures: (a) $x = 0.55$, $T = 5.9$ K; (b) $x = 0.65$, $T = 20.6$ K; (c) $x = 0.75$, $T = 65.2$ K and (d) $x = 0.80$, $T = 11$ K. The dashed line represents a fit to the (3 0 0) superstructure reflection, the dotted line the fit to the parasitic aluminum reflection from the sample holder. The solid line indicates the sum of both contributions.

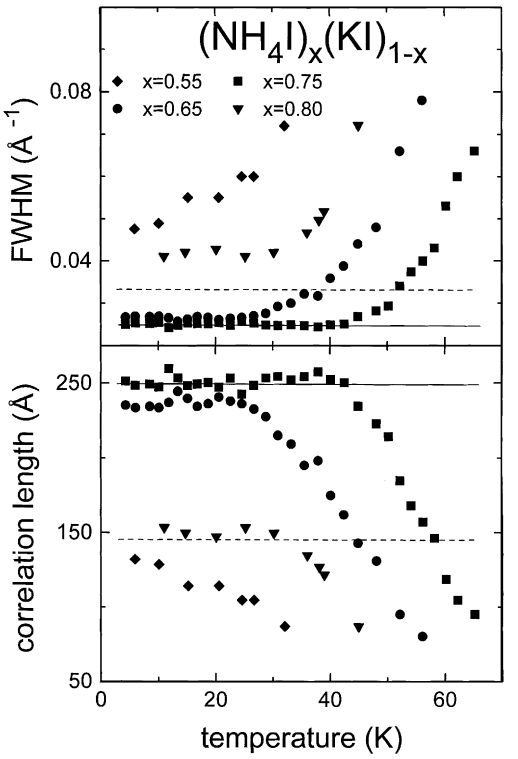

Fig. 4. Upper panel: Temperature dependence of the full-width at half- maximum of Q-scans for ammonium concentrations $x = 0.55$ (◆), 0.65 (●), 0.75 (■) and 0.80 (▼). The solid horizontal lines correspond to the experimental resolution. Lower panel: Correlation lengths versus temperature that have been calculated from the line widths are shown in the upper frame. For details see text. The horizontal lines correspond to correlation lengths limited by the experimental resolution.

(Fig. 3b), $x = 0.75$ (Fig. 3c) and $x = 0.80$ (Fig. 3d), only. Even at $T = 5.9$ K, the FWHM of the (3 0 0) reflection for $x = 0.55$ (Fig. 3a) significantly exceeds the experimental resolution, indicating a low-temperature state with SRO. We recall, that in the same crystal we could not detect traces of the ε-phase in the single-crystal diffraction experiment. From these results we can locate the stability of the ε-phase for concentrations 0.55 ($a = 7.172(2)$ Å) $< x \leqslant 0.80$ ($a = 7.225(3)$ Å) at low temperatures.

In Fig. 4 we present the main results of the fits to the elastic Q-scans. In the upper frame we plotted the FWHM as a function of temperature for all concentrations investigated. At low temperatures the line widths for $x = 0.65$, 0.75 (solid line) and 0.80 (dashed line) are resolution limited indicating LRO of the ε-phase. For $x = 0.55$ the FWHM exceeds the experimental resolution. On increasing temperatures the line widths of all samples increase. From these results we calculated the intrinsic correlation lengths. For a Gaussian-shaped line width the correlation length is given as $L_{\mathrm{corr}} = 2{*}\pi/(2{*}\ln\sigma)$, where $(2\ \ln\ \sigma)$ corresponds to the full-width at half-maximum. The results are shown in the lower panel of Fig. 4. At low temperatures and for ammonium concentrations $x = 0.65$, 0.75 and 0.80 the line widths and concomitantly the correlation lengths are limited by the instrumental resolution, indicated by a solid line for the 40′-20′-20′-30′ and a dashed line for the 60′-40′-40′-60′ configuration. For $x = 0.55$, even at the lowest temperatures

no true LRO within the ε-phase can be established. This regime, which can be characterized as a glassy state obviously is characterized by frozen-in SRO correlation, which exhibit the symmetry of the ε-phase and extends over 130 Å corresponding to domains or clusters of approximately 20 lattice constants along the cube axis.

With increasing temperatures all correlation lengths increase. For $x = 0.65$, 0.75 and 0.80 this happens when the structural phase-transition temperatures are approached. For $x = 0.55$ the FWHM steadily increases while the intensity decreases and for $T > 33$ K the quasielastic intensities at the (3 0 0) rlp cannot further be followed due to low intensities and large line widths.

3.2.3. *Quasielastic scans at the (3 0 0) reciprocal lattice point*

To study the relaxational dynamics in $(NH_4I)_x(KI)_{1-x}$ quasielastic scans were performed at the (3 0 0) rlp. This is the X-point of the Brillouin zone in the α-structure and it has been demonstrated by Berret et al. [16] on deuterated compounds and by Umeki et al. [17] on protonated compounds that diffusive scattering contributions appear at this rlp. Temperature-dependent energy-scans at $Q = (3\,0\,0)$ were followed in detail for the ammonium concentrations $x = 0.55$, 0.65, 0.75 and 0.80 in order to investigate systematically the evolution of line width and intensity. The line width measures the energy spread and provides direct experimental insight into the relaxation dynamics. In Fig. 5 representative constant-Q scans are shown for all ammonium concentrations investigated at some characteristic temperatures. First of all, we would like to focus on the spectra for $x = 0.65$ and 0.75. In a careful analysis we found out that neither a single Lorentzian nor a single Gaussian line shape gave a satisfactorily description of the experimental data. Even sophisticated fitting routines, which convolute the line shapes with the experimental resolution did not improve the fits significantly. Only a superposition of two contributions with different line widths and different temperature dependencies were able to fit the data and we found out that two Gaussians provided the best fits. Of course we are aware that for a quantitative analysis we have to use a jump-reorientational model to describe the relaxational motions of the NH_4^+-tetrahedra in the crystalline potential [18]. However, guided by a high-resolution TOF experiment [19], where we found that rotational jump models alone cannot describe the data, we tried to parametrize phenomenologically our data using two relaxation processes. This ansatz, to assume two different relaxation rates, also is in accordance with the observation of two dipolar relaxation modes in dielectric spectroscopy.

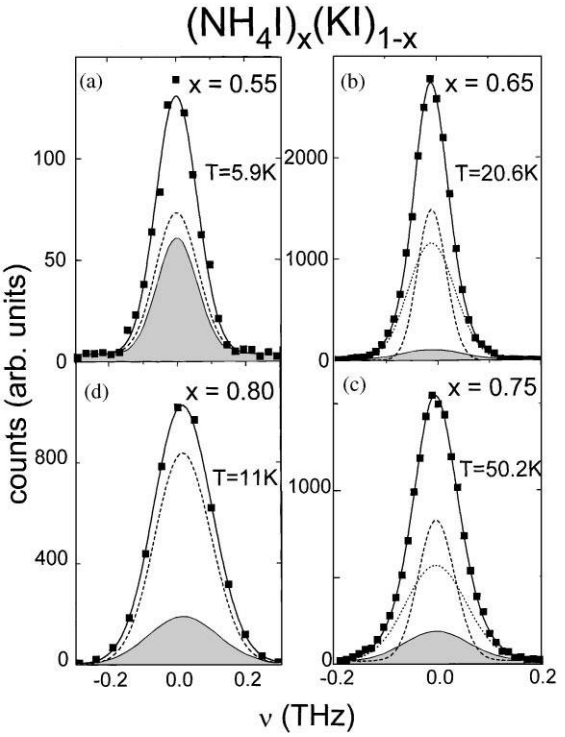

Fig. 5. Quasielastic scans at the (3 0 0) rlp at various temperatures for ammonium concentrations $x = 0.55$, 0.65, 0.75 and 0.80. The solid lines represent fits as described in the text. In (a) and (d) in addition to the quasielastic scattering from the mixed crystal (dashed line) the elastic incoherent background has been taken into account (shaded area). In (b) and (c) two Gaussian components had to be used to describe the quasielastic scattering contributions. Again, the shaded area indicates the incoherent background.

In the final analysis it was necessary to assume two Gaussian line shapes for $x = 0.65$ and 0.75. A third weak contribution, also with Gaussian line width, originates from the purely elastic scattering (shaded area). This contribution has been

determined from the purely elastic background at zero energy, off the (3 0 0) rlp and therefore, this third Gaussian component was fixed in intensity and line width during the fitting process. As mentioned before, this provides only a parametrization of the data and of course it would be much better to use a jump-reorientational model in addition to a second component. This procedure probably can be done with high-resolution data and a final analysis is in progress [19]. However, we certainly believe that two relaxation modes determine the quasielastic scattered intensity as shown for $x = 0.65$ (Fig. 5b) and $x = 0.75$ (Fig. 5c). The quasielastic scans for the samples with ammonium concentrations $x = 0.55$ (Fig. 5a) and $x = 0.80$ (Fig. 5d) can be fitted by a single Gaussian-shape function. For $x = 0.55$ this may be due to the vicinity to the glassy phase characterized by only one relevant time scale. For this concentration also the dielectric spectroscopy revealed one relaxation process, indicating that the two processes under consideration have merged. The results for $x = 0.80$ can be explained assuming that the time scale is too fast to be resolved in the present experiment. But it also may be due to the fact that the experiments on this mixed crystal were performed with a significantly relaxed resolution ($x = 0.80$) and therefore a clear separation into two components could not be performed.

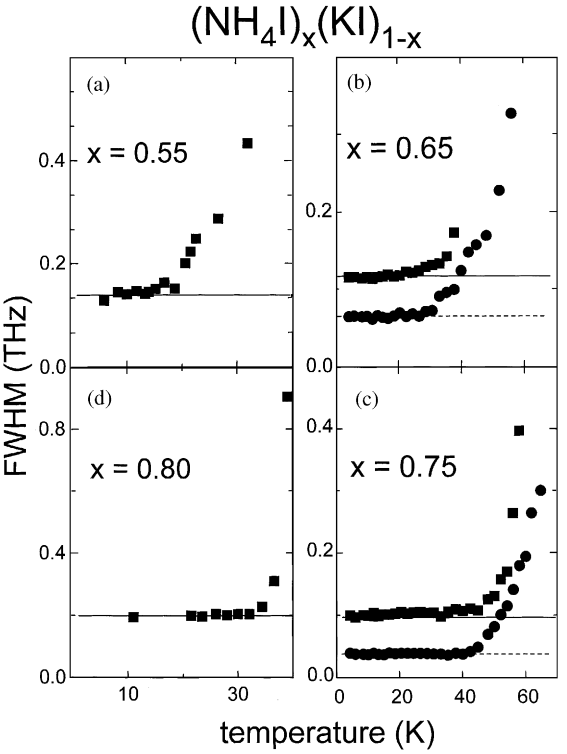

Fig. 6. Intensities of the constant-Q scans versus temperature for ammonium concentrations $x = 0.55, 0.65, 0.75$ and 0.80. The two components are indicated by the different symbols (● and ■).

Fig. 6a–d shows the temperature dependencies of the line widths for all concentrations investigated, which were derived from fits to Gaussian shapes as shown in Fig. 5. The two components observed in $x = 0.65$ (Fig. 6b) and 0.75 (Fig. 6c) are limited by two different experimental resolutions. One component which finally results in the (3 0 0) superlattice reflection is limited by the energy width of a scan through a well-defined Bragg reflection (indicated by a dashed line). The other component is limited by the quasielastic energy resolution which has been determined by a vanadium scan. Hence this component strictly represents a relaxational component. It is important to note that the "Bragg" component which appears well above the phase transition temperature appears at slightly higher temperatures. This observation provides first hints for a possible interpretation: one component arises from critical fluctuations related to the cubic (α-phase) to trigonal (ε-phase) phase transition. The other component most probably results from a reorientational motion of the ammonium tetrahedra. The quasielastic intensities as observed for $x = 0.55$ (Fig. 6a) and $x = 0.80$ (Fig. 6d) are limited by the pure quasielastic resolution. It indicates that both contributions do not result from static long-range structural order. SRO has been experimentally proven by the diffusive scans shown in the Figs. 3 and 4, but for $x = 0.80$ the correlation length of approximately 150 Å was determined by the experimental resolution. From the quasielastic scans we learn now that this order obviously is not truly static.

The temperature dependencies of the quasielastic intensities at the (3 0 0) rlp are shown for all concentrations in Fig. 7. On decreasing temperatures the intensities for $x = 0.80$ (solid squares in Fig. 7d)

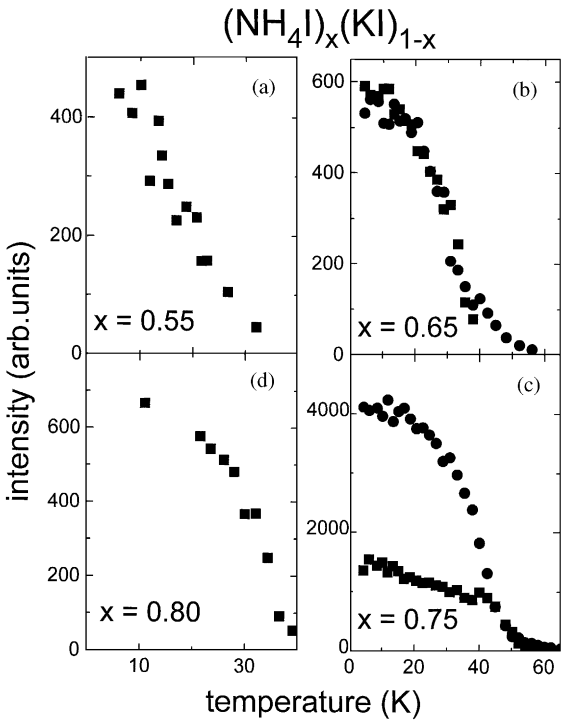

Fig. 7. Temperature dependence of the FWHM of constant-Q scans for ammonium concentrations $x = 0.55$, 0.65, 0.75 and 0.80. The two components for $x = 0.65$ and $x = 0.75$ are indicated by different symbols (● and ■). Dashed and solid lines indicate the experimental resolution for elastic and quasielastic scattering contributions, respectively.

smoothly increases, characteristic for the evolution of the order parameter at a second-order phase transition with a phase-transition temperature of $T_{\alpha\varepsilon} = 37$ K. The intensity follows a Brillouin-type function which saturates at low temperatures. A similar behavior is found for one component of the scattered intensities for $x = 0.65$ and $x = 0.75$ (solid circles in Fig. 7c and b). These contributions obviously originate from shifts of the center-of-mass lattice which finally establish the ε-phase. The phase-transition temperatures in these compounds are $T_{\alpha\varepsilon} = 38$ K for $x = 0.65$ and $T_{\alpha\varepsilon} = 47$ K for $x = 0.75$, slightly below the maximum of the dielectric loss as shown in Fig. 2. It is important to note, that the phase transition temperature for $x = 0.80$ is significantly lower than for $x = 0.75$. Precursor effects due to critical fluctuations for $T > T_{\alpha\varepsilon}$ were detected in all compounds, but certainly are strongest for $x = 0.65$. The second component, indicated by full squares, which has been observed in the samples $x = 0.65$ and $x = 0.75$, always appears just below the structural phase transition and steadily increases towards the lowest temperatures. From this systematic trends we immediately can identify the origin of the two contributions. The Brillouin-type functions describe critical fluctuations of the ε-phase at the X-point of the FCC lattice around the structural phase transition. For $T < T_{\alpha\varepsilon}$ these contributions result in the superlattice reflections of the ε-phase with LRO. The second contribution which appears at lower temperatures obviously originates from the slowing down of the reorientational motion of the NH_4^+-tetrahedra. Due to the structural distortions the local energy barriers become higher. This results in a slowing down of the molecular reorientations which then fall into the time window of the quasielastic neutron-scattering experiment. In the mixed crystals with ammonium concentrations $x = 0.55$ and $x = 0.80$ we observed only one component, most probably fluctuations due to short-range ordered clusters exhibiting the ε-phase. The slowing down of the ammonium molecules could not be identified. Possibly due to a strong translation–rotation coupling [20], their time scales are similar, an interpretation which is in accordance with the dielectric results. Another possibility is that the local distortions are not strong enough to create considerably enhanced energy barriers and therefore the molecular motion remains too fast to be detected with the given experimental resolution.

To our knowledge, so far two central peaks in structural phase transitions have been observed in Q-scans in the spiral antiferromagnet holmium [21] and in $SrTiO_3$ [22] indicating two different length scales. In both materials the two peaks were attributed to scattering from the surface and from the bulk. It has been speculated that two length scales correspond to two time scales [21]. We observed two different time scales, but definitely we believe that two different time scales will correspond to two different length scales in our system. Hence we wanted to exclude the possibility of surface effects. We systematically changed the size of the crystal thereby changing the ratio of bulk to surface area, but within experimental uncertainties

we always observed the same ration of the two quasielastic components. Hence we concluded that the origin of both peaks comes from the bulk material.

4. Discussion and conclusions

One important contribution of this communications is that we can construct an extended and improved x, T-phase diagram (Fig. 8). For a better comparison with other experimental work we present the characteristic temperatures as a function of the lattice parameters. We recall that a one-to-one correspondence with a x, T-phase diagram only exists under the asumption that Vegard's law holds. First of all we determined the concentration (lattice constant) regime where the trigonal ε-phase is the stable ground state. We found that for $x = 0.80$ the ε-phase evolves from the β-phase. This ε-phase is not truly static which possibly is due to the fact that in the martensitic αβ-phase transition the crystal broke up in a number of small domains which are far beyond the visible light, the crystal lost its transparency and got a milky color. This is the case for the $x = 0.80$ sample which goes throw the β-phase and subsequently reaches the ε-phase. Secondly, we have proven that the glassy regime of $(NH_4I)_x(KI)_{1-x}$ has to be subdivided in different regimes. The concentration regime which links up with the ε-phase at lower concentrations has to be characterized as ground state with frozen-in SRO trigonal distortions. At even lower ammonium concentrations and using dielectric spectroscopy [4], a spin-glass type of phase has been detected, characterized by frozen-in orientational disorder, but with the center-of-mass of the molecules fixed at an undistorted regular cubic lattice. Hence the mixed molecular system $(NH_4I)_x(KI)_{1-x}$ reveals in addition to the polymorphism at high ammonium concentrations, polyamorphism at low concentrations.

The second important result of this work is the observation of two quasielastic peaks corresponding to two time scales in the relaxation dynamics. Although we agree that this description is a mere parametrization of the experimental data, a rather plausible and straightforward explanation can be given: The two time scales appear in the ε-phase

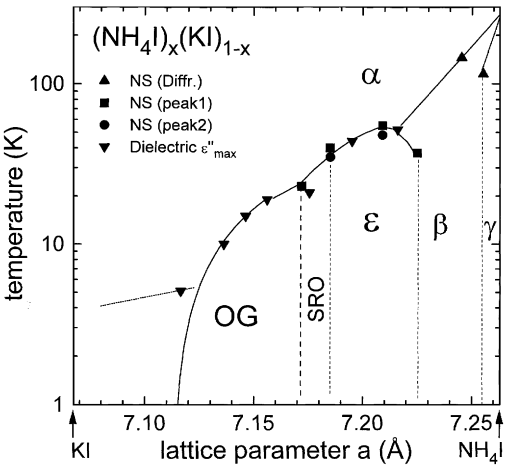

Fig. 8. The phase diagram of $(NH_4I)_x(KI)_{1-x}$. Here we plotted the phase transition temperatures versus the lattice parameter as determined from X-ray data. The circles and squares correspond to the triple-axis spectrometer results. The triangles (▼) represent the temperatures of the dielectric maximum and the triangles (▲) correspond to diffraction measurements taken from Ref. [6].

only. Recall that in this trigonal phase the ammonium molecules occupy two non-equivalent lattice sites. One sublattice reveals orientational order, while the other does not. The latter locally has a slightly distorted cubic environment. Hence we conclude that one time scale comes from the fluctuations close to the structural phase transition, which above the phase-transition temperature can be viewed as precursor effects of the trigonal distortions. The other time scale corresponds to the rotational motion of the ammonium tetrahedra from the orientationally disordered sublattice. Clearly these two relaxation rates can be well separated in the time/temperature scale. It seems that the reorientational motion drastically slows down at the structural phase transition. This effect most probably results from the local distortions which enhance the hindering barriers against reorientational jumps and from the dielectric results we know that the relaxation rates fall into the kHz regime at 10 K.

The question remains why we see only one relaxation process in the mixed crystal in the regime with SRO with an ammonium concentration $x = 0.55$. One possible explanation is that in this regime the reorientations are strongly coupled to the

dynamic structural displacements, and hence both relaxations are described by a very similar temperature dependence. This explanation seems to be in accordance with the dielectric results which reveal that the two relaxational processes have merged, at least in the low-frequency regime. The other possibility is that the molecular motion remains fast and the local environment of the ammonium tetrahedra is only slightly distorted which has been concluded from our single-crystal diffraction. It is clear, that for even lower ammonium concentrations the lattice remains cubic and only the relaxation dynamics of the ammonium tetrahedra survive. This has been exactly determined in dielectric experiments [4].

In conclusion, we have determined an improved phase diagram of the mixed molecular system $(NH_4I)_x(KI)_{1-x}$ (Fig. 8) revealing polymorphism and polyamorphism with a rich variety of different phases. At low temperatures and on decreasing ammonium concentrations the sequence α-, β-, γ- and ε-phase has been detected for $x > 0.55$, while at lower concentrations a short-range ordered "ε-glass" is followed by spin-glass type of frozen-in disorder. In addition to local structural distortions, the SRO state reveals also frozen-in orientational disorder. In the pure orientational glass the orientational degrees of freedom occupy regular cubic lattice sites but are frozen-in without long-range orientational order.

From quasielastic neutron scattering experiments we found experimental evidence for two relaxational processes which were identified as structural and orientational relaxations. We followed in detail the temperature evolution of the line widths and of the intensities of these relaxations and found that one component finally represent the truly static LRO of the ε-phase while the second component describes the slowing down of the molecular reorientations of one sublattice of the ε-phase.

Acknowledgements

We thank A. Maiazza for growing the high-quality single crystals. This project was partly supported by the BMBF under the contract number 03-LO5AU2-8.

References

[1] C.H. Perry, R.P. Lowndes, J. Chem. Phys. 51 (1969) 3648.
[2] N.G. Parsonage, L.A.K. Stavely, Disorder in Crystals, Clarendon Press, Oxford, 1978, p. 315.
[3] R. Havighurst, E. Mack, F.C. Blake, J. Am. Chem. Soc. 47 (1925) 29.
[4] M. Winterlich, R. Böhmer, A. Loidl, Phys. Rev. Lett. 75 (1995) 1783.
[5] M. Paasch, M. Winterlich, R. Böhmer, R. Sonntag, G.J. McIntyre, A. Loidl, Z. Phys. B 99 (1996) 333.
[6] M. Paasch, G.J. McIntyre, M. Reehuis, R. Sonntag, A. Loidl, Z. Phys. B 99 (1996) 339.
[7] C. Bostoen, G. Coddens, W. Wegener, J. Chem. Phys. 91 (1989) 6337.
[8] I. Fehst, R. Böhmer, W. Ott, A. Loidl, S. Haussühl, C. Bostoen, Phys. Rev. Lett. 64 (1990) 3139.
[9] U.T. Höchli, K. Knorr, A. Loidl, Adv. Phys. 39 (1990) 405.
[10] L. Vegard, Z. Phys. 5 (1921) 17.
[11] J.-F. Berret, S. Ravy, B. Hennion, J. Phys. I (France) 3 (1993) 1031.
[12] C. Wilkinson, H.W. Khamis, R.F.D. Stansfield, G.J. McIntyre, J. Appl. Crystallogr. 21 (1988) 471.
[13] V.F. Sears, Neutron-scattering lengths, in: A.J.C. Wilson (Ed.), International Tables for Crystallography, vol. C, Kluwer Academic Press, Dordrecht, 1992, p. 383.
[14] A. Loidl, K. Knorr, J.M. Rowe, G.J. McIntyre, Phys. Rev. B 37 (1988) 389.
[15] A. Loidl, T. Schräder, K. Knorr, R. Böhmer, B. Mertz, G.J. McIntyre, T. Vogt, H. Mutka, M. Müllner, H. Jex, S. Haussühl, Z. Phys.: Condens. Matter B 75 (1989) 81.
[16] J.-F. Berret, C. Bostoen, J.-L. Sauvajol, B. Hennion, S. Haussühl, Europhys. Lett. 16 (1991) 91.
[17] T. Umeki, K. Yagi, H. Terauchi, J. Phys. Soc. Jap. 63 (1994) 873.
[18] M. Bée, Quasielastic Neutron Scattering, Adam Hilger, Bristol, 1988.
[19] M. Ohl, F. Güthoff, R. Lechner, A. Loidl, submitted for publication.
[20] R.M. Lynden-Bell, K.H. Michel, Rev. Mod. Phy. 66 (3) (1994) 721.
[21] T.R. Thurston, G. Helgesen, D. Gibbs, J.P. Hill, B.D. Gaulin, G. Shirane, Phys. Rev. Lett. 70 (1993) 3151.
[22] G. Shirane, R.A. Cowley, M. Matsuda, S.M. Shapiro, Phys. Rev. B 48 (1993) 15595.